ELSEVIER

Journal of Organometallic Chemistry 531 (1997) 151–158

Journal of Organometallic Chemistry

Synthesis, characterization and in vitro antitumour activity of triphenyl- and tri-n-butyltin benzoates, phenylacetates and cinnamates

Rudolph Willem [a,b], Abdeslam Bouhdid [c], Bernard Mahieu [d], Laurent Ghys [a,b], Monique Biesemans [a,b], Edward R.T. Tiekink [e], Dick de Vos [f], Marcel Gielen [a,*]

[a] Faculty of Applied Sciences, Laboratory for General and Organic Chemistry (AOSC), Room 8G512, Free University of Brussels (V.U.B.), Pleinlaan 2, B-1050 Brussels, Belgium

[b] High Resolution NMR Centre, Free University of Brussels (V.U.B.), Pleinlaan 2, B-1050 Brussels, Belgium

[c] Faculty of Sciences, Free University of Brussels (V.U.B.), Pleinlaan 2, B-1050 Brussels, Belgium

[d] Catholic University of Louvain, INAN, B-1348 Louvain-la-Neuve, Belgium

[e] Department of Chemistry, The University of Adelaide, Adelaide, S.A. 5005, Australia

[f] Medical Department, Pharmachemie BV, NL-2003 RN Haarlem, Netherlands

Received 9 July 1996

Abstract

Spectroscopic, structural and antitumour properties of triphenyltin and tri-n-butyltin benzoates, phenylacetates and cinnamates are compared with those of their corresponding pentafluorophenyl analogues.

Keywords: Tin carboxylate; Anti cancer; Nuclear magnetic resonance; Crystal structure; Mössbauer spectroscopy; X-ray diffraction

1. Introduction

Condensation compounds of diorganotin oxides with mono- [1], di- [2], tri-, tetra- [3] and pentafluorobenzoic acids [4] exhibit significant in vitro antitumour activities [5]. Triorganotin pentafluorobenzoates, -phenylacetates and -cinnamates are likewise active [6].

We synthesized triphenyltin and tri-n-butyltin benzoates, phenylacetates and cinnamates in order to compare their chemical properties and antitumour activities with those of the corresponding pentafluorophenyl analogues. This study aims to assess the influence of substituting a phenyl group for a pentafluorophenyl one in a series of triorganotin carboxylates.

Triphenyltin and tri-n-butyltin cinnamates [7], as well as triphenyltin benzoate [8,9], have been synthesized previously. Some additional structural data, as well as their antitumoural activity in vitro are presented in this paper, in addition to the characterisation of the other compounds. A comparison of their structural and biological activities with those of their pentafluorophenyl analogues is included.

* Corresponding author.

2. Results and discussion

2.1. Syntheses

The compounds synthesized obey the general formula H_5C_6–Z–CO_2SnR_3, where R = n-butyl or phenyl and Z is either absent or a CH_2 or CH=CH moiety (see Fig. 1). Physical characteristics are collected in Table 1.

The compounds were obtained by condensation of the appropriate carboxylic acid with either tri-n-butyltin acetate [10–12] or triphenyltin hydroxide [8,13] in toluene/ethanol (4:1) under water elimination.

2.2. ^{119}Sn Mössbauer data

The Mössbauer parameters of the $H_5C_6CO_2SnR_3$, $H_5C_6CH_2CO_2SnR_3$ and $H_5C_6CH{=}CHCO_2SnR_3$ compounds are listed in Table 2.

The quadrupole splittings QS are found in the range 3.60–3.72 mm s^{-1} except for triphenyltin benzoate having a value of 2.46 mm s^{-1} (lit. 2.55 mm s^{-1} [8]). Furthermore, the QS value observed for tri-n-butyltin benzoate is 0.32 mm s^{-1} smaller than the one found for its pentafluorobenzoate analogue. This difference is only

PII S0022-328X(96)06686-7

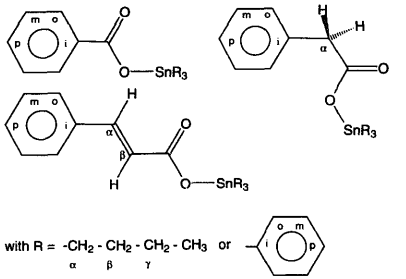

Fig. 1. Atom labelling scheme of the triphenyl- and tri-n-butyltin benzoates, phenylacetates and cinnamates.

0.11 mm s^{-1} for the phenylacetate and 0.12 mm s^{-1} for the cinnamate. The electron withdrawing effect of the perfluorophenyl groups is responsible for an enhanced imbalance in the electronic distribution around the tin nucleus. As a consequence, the electronic field gradient is increasing, in agreement with the observation of a larger quadrupole splitting in the fluorinated compounds [6]. Insertion of the $-CH_2$(phenylacetate) or $-CH=CH-$ (cinnamate) group reduces the influence of the electronegative F atoms, the distance between the tin atom and the perfluorophenyl group increasing.

Values of *QS* in the range 3.0–4.1 mm s^{-1} are typical for polymeric five-coordinate structures [8,13–15] with a planar SnR_3 unit and two apical carboxylate oxygen atoms. By contrast, *QS* values in the range 2.36–2.97 are characteristic of monomeric structures. Therefore, the compounds are polymeric with a five-coordinate tin atom in the solid state, up to triphenyltin benzoate [8] which is monomeric. ^{117}Sn CP-MAS NMR and X-ray crystallographic data (see below) confirm this. The monomeric nature of triphenyltin benzoate is detailed by the X-ray diffraction study presented below. It is in contrast with the polymeric nature of triphenyltin perfluorobenzoate, in which the coordination expansion is favoured by the enhanced Lewis acidity of the tin atom. The latter is presumably induced by the stronger electron withdrawing nature of the perfluorobenzoate moiety compared with the benzoate one.

The isomer shifts are found in the range 1.44–1.48 mm s^{-1} for the tri-n-butyltin compounds and in the range 1.25–1.30 mm s^{-1} for the triphenyltin species. The tri-n-butyl- and triphenyltin benzoates exhibit isomer shifts that are, respectively, 0.05 and 0.09 mm s^{-1} smaller than their pentafluorophenyl analogues. In contrast, the phenylacetates and cinnamates display similar values within experimental error. Isomer shifts are closely related to the s-electronic density at the nucleus; lowering the s-density results in a decrease of the isomer shift. Oxygen atoms bound to tin use $p\pi d\pi$

Table 1
Melting points, recrystallization solvents and yields for the triphenyltin and tri-n-butyltin benzoates, phenylacetates and cinnamates

Compound	M.p. (°C)	Recrystallization solvent	Yield (%)
$H_5C_6CO_2SnBu_3$	b.p. 114 °C/1 mmHg	—	91
$H_5C_6CH_2CO_2SnBu_3$	56–57	CH_2Cl_2/hexane	90
$H_5C_6CH{=}CHCO_2SnBu_3$	75–76	CH_2Cl_2/hexane	91
	lit. [7] 74–76		
$H_5C_6CO_2SnPh_3$	86–87	C_2H_5OH	86
	lit. [8] 85–87		
$H_5C_6CH_2CO_2SnPh_3$	139–141	C_2H_5OH	81
$H_5C_6CH{=}CHCO_2SnPh_3$	138–140	C_2H_5OH	85
	lit. [7] 138–139		

Table 2
^{119}Sn Mössbauer parameters, *QS* (quadrupole splitting), *IS* (isomer shift relative to calcium stannate) and line widths (Γ_1 and Γ_2) (mm s^{-1}) for tri-n-butyl and triphenyltin benzoates, phenylacetates and cinnamates. For comparison, the *IS* and *QS* values obtained for the corresponding pentafluorinated analogues are given in parentheses

Compound	*IS*	*QS*	Γ_1	Γ_2
H_5C_6–CO_2SnBu_3	1.48 (1.53)	3.65 (3.97)	0.95	0.94
H_5C_6–CH_2–CO_2SnBu_3	1.45 (1.48)	3.72 (3.83)	0.87	0.94
H_5C_6–CH=CH–CO_2SnBu_3	1.44 (1.45)	3.63 (3.75)	0.88	0.95
	lit. [7] 1.45	lit. [7] 3.65	lit. [7] 0.96	lit. [7] 0.97
H_5C_6–CO_2SnPh_3	1.25 (1.34)	2.46 (3.76)	0.93	0.82
	lit. [8] 1.24	lit. [8] 2.55		
H_5C_6–CH_2–CO_2SnPh_3	1.30 (1.31)	3.60 (3.55)	0.78	0.78
H_5C_6–CH=CH–CO_2SnPh_3	1.30 (1.31)	3.60 (3.52)	0.78	0.78
	lit. [7] 1.31	lit. [7] 3.61	lit. [7] 0.88	lit. [7] 0.87

bonding to some extent, which brings about a screening effect of 5d against 5s electrons. Reduction of the s-electron density resulting from the withdrawing power of the pentafluorophenyl group lowers this screening effect and thereby enhances the isomer shift. This effect becomes negligible when the electron withdrawing pentafluorophenyl group is too far from the tin–oxygen bond, as is the case in phenylacetates and cinnamates.

2.3. Crystal structure of $H_5C_6CO_2SnPh_3$

The molecular structure of $H_5C_6CO_2SnPh_3$ is shown in Fig. 2 and selected interatomic parameters are listed in Table 3. The structure is in agreement with the *QS* value found by Mössbauer spectroscopy. The lattice is comprised of discrete molecules of the compound with the closest non-hydrogen intermolecular contact of 3.461(5) Å occurring between the O(2) and C(25)′ atoms (symmetry operation x, $0.5-y$, $-0.5+z$). The tin atom exists in a distorted tetrahedral geometry defined by three *ipso*-C atoms of the phenyl groups and the O(1) atom [Sn–O(1) 2.073(3) Å] of the benzoate. The major distortion from the ideal tetrahedral geometry is found in the O(1)–Sn–C(8) angle of 94.8(1)°. The relatively close presence of the O(2) atom, i.e. Sn···O(2) is 2.674(3) Å, does not disrupt the O(1)–Sn–C(14) and O(1)–Sn–C(20) angles significantly (i.e. 109.8(1)° and 110.2(1)° respectively), however, it is noteworthy that the C(14)–Sn–C(20) angle of 119.4(2)° is the next major distortion from the ideal geometry. The monodentate mode of coordination of the benzoate is reflected in the disparate C(1)–O(1) and C(1)–O(2) bond distances of 1.316(5) and 1.226(5) Å respectively, with the longer separation being associated with the stronger Sn–O(1) interaction. The structural motif reported here for $H_5C_6CO_2SnPh_3$ is one of the two major motifs found for compounds of the general formula $R'CO_2SnR_3$, the other being the *trans*-R_3SnO_2 motif [16].

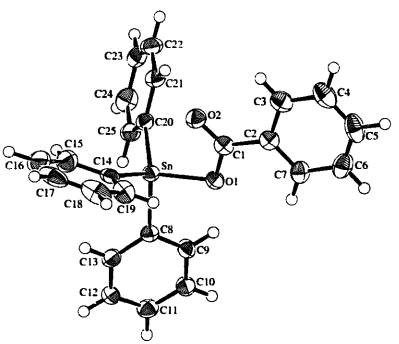

Fig. 2. Molecular structure and crystallographic numbering scheme for $H_5C_6CO_2SnPh_3$.

Table 3
Selected bond distances (Å) and angles (°) for $H_5C_6CO_2SnPh_3$

Sn–O(1)	2.073(3)	Sn–C(8)	2.139(3)
Sn–C(14)	2.108(4)	Sn–C(20)	2.138(4)
C(1)–O(1)	1.316(5)	C(1)–O(2)	1.226(5)
C(1)–C(2)	1.478(6)		
O(1)–Sn–C(8)	94.8(1)	O(1)–Sn–C(14)	109.8(1)
O(1)–Sn–C(20)	110.2(1)	O(1)–Sn–C(14)	112.0(2)
C(8)–Sn–C(20)	107.9(2)	C(8)–Sn–C(14)	119.4(2)
Sn–O(1)–C(1)	105.6(3)	O(1)–C(1)–O(2)	120.8(4)
O(1)–C(1)–C(2)	116.9(4)	O(2)–C(1)–C(2)	122.4(4)
Sn–C(8)–C(9)	120.6(3)	Sn–C(8)–C(13)	121.7(3)
Sn–C(14)–C(15)	120.2(4)	Sn–C(14)–C(19)	122.1(3)
Sn–C(20)–C(21)	123.6(3)	Sn–C(20)–C(25)	116.7(3)

2.4. ^1H NMR data

The ^1H NMR data of $H_5C_6CO_2SnR_3$, $H_5C_6CH_2CO_2SnR_3$ and $H_5C_6CH{=}CHCO_2SnR_3$ are shown in Table 4.

The proton chemical shift assignment of the tri-n-butyltin moiety could be achieved from the ^1H NMR spectrum at 500 MHz, well-resolved multiplets being observed, in contrast to the strongly overlapping and non-first-order pattern of the spectrum at 250 MHz.

The ^1H chemical shift ranges of the triphenyltin moiety were deduced mainly from resonance intensities and, where appropriate, from the presence of $^3J(^1H-^{119/117}Sn)$ coupling satellites and/or $^3J(^1H-^1H)$ multiplets. Some of the $^nJ(^1H-^{119/117}Sn)$ coupling constants were determined from $^1H-^{119}Sn$ HMQC experiments [17].

2.5. ^{13}C NMR data

The ^{13}C NMR data of $H_5C_6CO_2SnR_3$, $H_5C_6CH_2CO_2SnR_3$ and $H_5C_6CH{=}CHCO_2SnR_3$ are given in Table 5 (R = n-butyl) and Table 6 (R = phenyl). The assignment of the ^{13}C resonances of the tri-n-butyltin part is straightforward from the $^nJ(^{13}C-^{119/117}Sn)$ coupling constants. The aromatic resonances of the triphenyltin moieties are easily assigned on the basis of both aromatic $^nJ(^{13}C-^{119/117}Sn)$ coupling constants and signal intensities [9].

The discrimination between the ^{13}C resonances of the *ortho* and *meta* carbon atoms of the phenyl group of the cinnamate moiety necessitated $^1H-^{13}C$ HMBC experiments [19] for both triorganotin compounds as well as for the cinnamic acid itself. For the other compounds, the assignment of the resonances of the phenyl group of the carboxylate moiety was straightforward from aromatic ^{13}C chemical shift increments [18].

Table 4
^{1}H NMR data in $CDCl_3$ for tri-n-butyl- and triphenyltin benzoates, phenylacetates and cinnamates; chemical shifts in ppm with respect to TMS; $^nJ(^1H-^1H)$ coupling constants in Hz in square brackets; unresolved $^nJ(^1H-^{117/119}Sn)$ coupling constants in bold in braces; bd, broad doublet; d, doublet, dd, doublet of doublets; m, complex pattern; s, singlet; t, triplet; tq, triplet of quartets; tt, triplet of triplets

Compound	$Bu_3SnO_2C-C_6H_5$	$Bu_3SnO_2CCH_2-C_6H_5$ [a]	$Bu_3SnO_2CCH=CH-C_6H_5$
H_o	bd: 8.07 [7.3]	m: 7.18–7.28	dd: 7.48 [7.6, 2.1]
H_m	dd: 7.38 [7, 7]	m: 7.18–7.28	m: 7.32–7.38
H_p	t: 7.45 [7]	m: 7.18–7.28	m: 7.32–7.38
Ph–CHα	—	s: 3.59	d: 7.60 [15.9] [c]
=CHβ	—	—	d: 6.46 [15.9] [c]
$SnCH_2(\alpha)$	m: 1.23–1.42	t: 1.21 [8] {53} [b]	t: 1.30 [7.0] {53}
$-CH_2(\beta)$	tt: 1.66 [7, 7] {63}	tt: 1.55 [8, 8] {66} [b]	tt: 1.62 [7, 7] {63}
$-CH_2(\gamma)$	m: 1.23–1.42	tq: 1.28 [7, 7]	tq: 1.34 [7, 7]
$-CH_3$	t: 0.91 [7.2]	t: 0.87 [7.4]	t: 0.91 [7.2]
Compounds	$Ph_3SnO_2C-C_6H_5$	$Ph_3SnO_2CCH_2-C_6H_5$	$Ph_3SnO_2CCH=CH-C_6H_5$
H_o	dd: 8.23 [7.3, 1.5]	m: 7.23–7.28	m: 7.48–7.52
H_m	m: 7.44–7.57	m: 7.23–7.28	m: 7.34–7.36
H_p	m: 7.44–7.57	m: 7.23–7.28	m: 7.48–7.52
Ph–CHα	—	s: 3.71	d: 7.74 [15.9] [c]
=CHβ	—	—	d: 6.56 [15.9] [c]
H_o (PhSn)	m: 7.87–7.90 [d]	m: 7.64–7.68 [d]	m: 7.75–7.80 [d]
H_{m+p} (PhSn)	m: 7.44–7.57	m: 7.34–7.53	m: 7.40–7.50

[a] Determined from a 500 MHz spectrum.
[b] $^nJ(^1H-^{119}Sn)$ determined from the $^1H-^{119}Sn$ HMQC spectrum.
[c] Assignment from a $^1H-^{13}C$ HMBC spectrum recorded at 500 MHz.
[d] Rough estimation of the unresolved $^3J(^1H-^{119/117}Sn)$ coupling constant for the *ortho* protons: 60 ± 4 Hz.

Holecek, Tiekink and coworkers [9,20–24] have shown that $^1J(^{13}C-^{119}Sn)$ coupling constants are good indicators of the coordination number of the tin atom in triorganotin compounds. Four-coordinate triphenyltin compounds exhibit couplings in the range 550–650 Hz and five-coordinate triphenyltin compounds in the range 750–850 Hz. By contrast, four-coordinate tri-n-butyltin compounds exhibit $^1J(^{13}C-^{119}Sn)$ coupling constants in the range 325–390 Hz and five-coordinate ones in the range 440–540 Hz.

All the triorganotin carboxylates of this investigation exhibit $^1J(^{13}C-^{119}Sn)$ coupling constants in solution characteristic of tetrahedral compounds, being of the order of 358 Hz in the tri-n-butyltin compounds (see

Table 5
^{13}C NMR data in $CDCl_3$ for tri-n-butyltin benzoate, phenylacetate and cinnamate; chemical shifts in ppm with respect to TMS; aromatic chemical shifts of the free acids in parentheses (from Ref. [18] for the benzoic and phenylacetic acids; the data on free cinnamic acid are from this work); $^nJ(^{13}C-^{119/117}Sn)$ coupling constants in square brackets (a single approximate value is given when they are unresolved)

Compound	$Bu_3SnO_2C-C_6H_5$	$Bu_3SnO_2CCH_2-CH_6H_5$	$Bu_3SnO_2CCH=CH-C_6H_5$
C_i	nv (130.6)	135.7 (132.7)	135.0 (134.2)
C_o	130.2 (130.1)	128.4 (128.9)	127.9 [a] (128.4)
C_m	128.0 (128.4)	129.3 (129.7)	128.8 [a] (129.0)
C_p	132.1 (133.7)	126.6 (127.6)	129.8 (130.8)
Ph–Cα	—	42.1 (41.0)	144.0 (147.1)
=Cβ	—	—	119.9 (115.1)
C=O	171.6 (168.0)	176.9 (178.4)	172.0 (172.7) lit. [7] 172.1
$Sn-CH_2(\alpha)$	16.6 [358/341]	16.5 [359/342]	16.6 [357/340] lit. [7] 16.6 [359]
$-CH_2(\beta)$	27.8 [20]	27.8 [20]	27.9 [20] lit. [7] 27.9 [20.6]
$-CH_2(\gamma)$	26.9 [65/63]	26.9 [64]	27.1 [65] lit. [7] 27.1 [64.5]
$-CH_3$	13.6	13.6	13.6 lit. [7] 13.7

[a] Assignment from $^1H-^{13}C$ HMBC spectrum.
nv: resonance hidden under C_o or C_m resonance.

Table 6
^{13}C NMR data in $CDCl_3$ for triphenyltin benzoate, phenylacetate and cinnamate; for further details, see caption to Table 5

Compound	$Ph_3SnO_2C-C_6H_5$	$Ph_3SnO_2CCH_2-C_6H_5$	$Ph_3SnO_2CCH=CH-C_6H_5$
C_i	129.0 (130.6)	135.1 (132.7)	134.8 (134.2)
C_o	130.7 (130.1) lit. [9] 130.1	128.4 (128.9)	128.2 [a] (128.4)
C_m	128.3 (128.4) lit. [9] 128.1	129.4 (129.7)	128.9 [a] (129.0)
C_p	132.8 (133.7) lit. [9] 132.6	126.8 (127.6)	130.1 (130.8)
Ph–Cα	—	41.3 (41.0)	145.6 (147.1)
=Cβ	—	—	118.4 (115.1)
C=O	173.1 (168.0) lit. [9] 172.8	178.2 (178.4)	173.4 (172.7) lit. [7] 173.2
C_i (PhSn)	138.5 [650/620] lit. [9] 138.2 [$^1J(^{13}C-^{119}Sn)$ = 648.4]	138.2 [647] [$^1J(^{13}C-^{119}Sn)$ = 649.4]	138.6 [$^1J(^{13}C-^{117}Sn)$ = 617] [b] lit. [7] 138.4
C_o (PhSn)	137.0 [49] lit. [9] 136.8 [48.4]	136.9 [50/48]	137.0 [49/47] lit. [7] 136.9 [48.9]
C_m (PhSn)	129.0 [65/62] lit. [9] 128.8 [64.4]	128.9 [60/57]	129.0 [65/62] lit. [7] 128.9 [63.5]
C_p (PhSn)	130.2 [13] lit. [9] 130.9 [13.6]	130.2 [13]	130.3 [14] lit. [7] 130.1

[a] Assignment from $^1H-^{13}C$ HMBC spectrum.
[b] $^1J(^{13}C-^{117}Sn)$ coupling constant determined from the ^{117}Sn NMR spectrum.

Table 5) and 650 Hz in the triphenyltin ones (see Table 6) [9,24,25]. The polymeric structure evidenced by the Mössbauer and ^{117}Sn NMR data (see below) in the solid state (except for triphenyltin benzoate, see above) is therefore lost in solution to generate a monomeric tetrahedral structure.

The ^{13}C chemical shift of the *ipso*-carbons of the triphenyltin moiety around 138 ppm (see Table 6) observed in solution is also characteristic of a tetrahedral tin atom [24], since five-coordinate triphenyltin carboxylates show a value approximately 4 ppm at higher frequency.

2.6. ^{117}Sn NMR data

The ^{117}Sn NMR spectra of the tri-n-butyl- and triphenyltin compounds in $CDCl_3$ solution exhibit a single resonance in the range characteristic for tetrahedral compounds, between −109.0 and −114.5 ppm for the triphenyltin compounds and between 107.9 and 110.7 ppm for the tri-n-butyltin derivatives (see Table 7) [20]. This confirms the four-coordination in solution proposed from the ^{13}C data. Indeed, the ^{119}Sn chemical shifts of five-coordinate triphenyltin and tri-n-butyltin compounds range from −180 to −280 ppm and +40 to −60 ppm respectively [20].

Except for triphenyltin benzoate, that is found to be four-coordinate in both the solid state [8] and $CDCl_3$ solution [9], the isotropic chemical shifts obtained by ^{117}Sn CP-MAS NMR (see Table 7) in the crystalline state, characteristic of five-coordination at tin, indicate a polymeric structure being lost in solution towards a tetrahedral configuration. It is well established that polymeric or oligomeric organotin structures, present in the solid state and/or in concentrated solutions, can decompose to their monomers upon dilution [10,25]. The results obtained for the pentafluorophenyl analogues of the above compounds are comparable [6], except that triphenyltin perfluorobenzoate is five- and not four-coordinate in the solid state.

2.7. *In vitro antitumour screening*

The results of the in vitro antitumour screening of the six triorganotin carboxylates against a selected panel of six human tumour cell lines, MCF-7 and EVSA-T, two breast tumours, WiDr, a colon carcinoma, IGROV, an ovarian cancer, M19 MEL, a melanoma, and A498, a

Table 7
^{117}Sn NMR data in $CDCl_3$ and ^{117}Sn CP-MAS NMR data in the solid state for tri-n-butyl- and triphenyltin benzoates, phenylacetates and cinnamates; chemical shifts in ppm ($\Xi(^{117}Sn = 35.632295$ [26])

Compound	δ (^{117}Sn) ($CDCl_3$)	δ (^{117}Sn) (solid state)
$H_5C_6-CO_2SnBu_3$	110.3	—
$H_5C_6-CH_2-CO_2SnBu_3$	110.7	−48
$H_5C_6-CH=CH-CO_2SnBu_3$	107.9 lit. [7] 109.4	−55
$H_5C_6-CO_2SnPh_3$	−111.7	−117
$H_5C_6-CH_2-CO_2SnPh_3$	−109.0 lit. [9] −109.9	−288
$H_5C6-CH=CH-CO_2SnPh_3$	−114.5 lit. [7] −113.5	−261

Table 8
In vitro antitumour activities (ID_{50} (ng ml^{-1})) against MCF-7 and EVSA-T, two breast cancers, WiDr, a colon cancer, IGROV, an ovarian cancer, M19 MEL, a melanoma, and A498, a renal cancer, of tri-n-butyl- and triphenyltin benzoates, phenylacetates and cinnamates; the values of the corresponding pentafluorobenzoates, -phenylacetates and -cinnamates [6] as well as some reference compounds [27] used clinically

Compound	MCF-7	EVSA-T	WiDr	IGROV	M19 MEL	A498
$Bu_3SnO_2C-C_6F_5$ [6]	15	< 3	20	25	60	50
$Bu_3SnO_2CCH_2-C_6F_5$ [6]	14	< 3	12	12	52	51
$Bu_3SnO_2CCH=CH-C_6F_5$ [6]	13	< 3	14	11	45	54
$Bu_3SnO_2C-C_6H_5$	130	15	70	100	110	190
$Bu_3SnO_2CCH_2-C_6H_5$	42	11	50	50	85	75
$Bu_3SnO_2CCH=CH-C_6H_5$	23	< 3	45	38	47	63
$Ph_3SnO_2C-C_6F_5$ [6]	45	17	90	44	130	120
$Ph_3SnO_2CCH_2-C_6F_5$ [6]	14	6	17	20	18	30
$Ph_3SnO_2CCH=CH-C_6F_5$ [6]	20	9	30	34	40	37
$Ph_3SnO_2C-C_6H_5$	650	110	500	470	800	950
$Ph_3SnO_2CCH_2-C_6H_5$	4	< 3	5	5	13	21
$Ph_3SnO_2CCH=CH-C_6H_5$	12	3	22	16	30	52
Carboplatin [27]	10500	4500	3500	2400	5500	18000
cis-Platin [27]	1400	920	1550	230	780	1200
5-Fluorouracil [27]	350	720	440	850	310	340
Methotrexate [27]	15	26	7	20	18	16
Doxorubicin [27]	25	13	18	150	21	55

renal cancer, are presented in Table 8. They are compared with those of their pentafluorophenyl analogues described previously [6]. The values of some clinically used reference compounds are also given for comparison [27].

The three tri-n-butyltin compounds are significantly more active or at least of the same order of activity against all cell lines when compared with carboplatin, *cis*-platin or 5-fluorouracil [27]. The tri-n-butyltin and triphenyltin cinnamates are especially active against EVSA-T. The non-fluorinated triorganotin benzoates of this study are less to much less active than their pentafluorinated analogues. The cinnamates display, in contrast, generally comparable activities, being pentafluorinated or not. The tri-n-butyltin phenylacetate is slightly less active than its pentafluorinated analogue; however, the non-fluorinated triphenyltin phenylacetate appears to be the most active compound of the whole series. A number of conclusions can be drawn from the data presented in Table 8.

The differences in activity for the benzoates are correlated to the higher Sn–O bond lability in the perfluorobenzoates compared with the non-fluorinated ones, as a consequence of the stronger electron withdrawing character of the C_6F_5 group compared with the C_6H_5 group. By contrast, in the cinnamates and phenylacetates, the triorganotin moieties are determinant for the high activity, the fluorination of the phenyl group having almost no influence; the latter is too far away from the tin atom to exert an electronic influence. It is noteworthy that other fluorinated phenylacetates have been shown to be quite active [4], providing evidence that this moiety can cause favourable antitumour activities in organotin compounds.

3. Experimental part

3.1. Syntheses

3.1.1. Tri-n-butyltin compounds

Equimolar quantities of tri-n-butyltin acetate and benzoic, phenylacetic or cinnamic acid are dissolved in a toluene/ethanol (4:1) mixture in a 250 ml flask equipped with a Dean–Stark funnel. This mixture is refluxed for 4 to 6 h. The ternary and subsequent binary azeotropes are distilled off up to 50% of the initial solvent volume. The remaining solution is evaporated and the product obtained is recrystallized from an appropriate solvent (see Table 1).

3.1.2. Triphenyltin compounds

Similarly an equimolar mixture of triphenyltin hydroxide and a suitable carboxylic acid are reacted and the desired compounds isolated and purified as above (see Table 1).

3.2. Instrumental methods

3.2.1. Standard 1D and 2D NMR experiments

All NMR spectra were recorded from $CDCl_3$ solutions on a Bruker AC250 spectrometer, using a QNP probe tuned at 250.13, 62.93 and 89.15 MHz for ^1H, ^{13}C and ^{117}Sn nuclei respectively. ^1H and ^{13}C resonances were referenced to the solvent peak at 7.24 and 77.0 ppm respectively, while $\Xi(^{117}Sn) = 35.632295$ [26]

was used for the ^{117}Sn resonances. For the one proton spectrum (see Table 4) a Bruker AMX500 spectrometer was used. The $^{1}H-^{119}Sn$ HMQC and $^{1}H-^{13}C$ HMBC spectra were recorded as described elsewhere [17].

3.2.2. CP-MAS ^{117}Sn spectra

All CP-MAS NMR spectra [28] were recorded on a Bruker AC250 spectrometer, operating at 89.15 MHz for the ^{117}Sn nucleus, interfaced with an Aspect 3000 computer and equipped with a MAS broad-band probe for solid state experiments. The matching condition for Hartmann–Hahn cross-polarization [28] (^{1}H 90° pulse length 5 ms) and the chemical shift reference were set with (*cyclo*-$C_6H_5)_4Sn$ for the ^{117}Sn nucleus [29] [−97.35 ppm relative to $(CH_3)_4Sn$]. 7 mm OD ZrO_2 rotors were used. The ^{117}Sn spectra were typically obtained by acquiring 32K data points over a spectral width of 166.7 kHz, a 2 ms contact time and a relaxation delay of 2 s with 1000 to 10000 scans. The isotropic ^{117}Sn chemical shifts were found from spectra recorded at two or three different spinning rates [28].

^{117}Sn rather than the more common ^{119}Sn spectra were recorded in order to overcome a local radio interference problem [30]. $^{117}Sn/^{119}Sn$ isotopic effects on tin chemical shifts are known to be negligible [31].

3.2.3. Mössbauer spectroscopy

Mössbauer spectra were obtained as described previously [32].

3.2.4. Crystallography

Intensity data for a colourless crystal were measured at −100 °C on a Rigaku AFC6R diffractometer fitted with Mo Kα radiation ($\lambda = 0.71073$ Å; graphite monochromator) employing the ω:2θ scan technique. Data were corrected for Lorentz and polarization effects [33] and for absorption using a procedure based on psi-scans [34]. The structure was solved by direct methods [35] and refined by a full-matrix least-squares procedure based on F^2 employing all reflections [33]. Non-hydrogen atoms were refined with anisotropic thermal parameters and hydrogen atoms were included in the model at their calculated positions (C–H 0.97 Å). A sigma weighting scheme (i.e. $1/\sigma^2(F_o)$) was applied and the refinement was continued until convergence. The molecular structure is illustrated in Fig. 2 [36], crystal data and final refinement details are given in Table 9 and fractional atomic coordinates are listed in Table 10. Additional crystallographic details can be obtained from ERTT.

Table 9
Crystallographic data for $H_5C_6CO_2SnPh_3$

Formula	$C_{25}H_{30}O_2Sn$
Formula weight	471.1
Crystal size (mm^3)	0.11×0.24×0.40
Crystal system	monoclinic
Space group	$P2_1/c$
a (Å)	11.132(3)
b (Å)	12.250(4)
c (Å)	15.165(3)
β (°)	92.39(2)
V ($Å^3$)	2066.1(9)
D_{calc} ($g\,cm^{-3}$)	1.514
$F(000)$	944
Z	4
μ (cm^{-1})	12.53
Transmission coefficients	0.830–1.0
No. of data collected	5239
θ_{max} (°)	27.5
No. of unique data	4994
No. of refined parameters	253
R	0.068
R_w	0.083
Residual density ($e\,Å^{-3}$)	0.83

Table 10
Fractional atomic coordinates for $H_5C_6CO_2SnPh_3$

Atom	x	y	z
Sn	−0.24785(2)	0.25131(3)	0.41548(2)
O(1)	−0.3155(3)	0.3756(2)	0.3350(2)
O(2)	−0.1432(3)	0.3355(3)	0.2752(2)
C(1)	−0.2337(4)	0.3926(4)	0.2764(3)
C(2)	−0.2554(4)	0.4839(4)	0.2141(3)
C(3)	−0.1663(4)	0.5129(4)	0.1584(3)
C(4)	−0.1839(5)	0.6013(4)	0.1009(3)
C(5)	−0.2893(6)	0.6589(4)	0.1005(3)
C(6)	−0.3779(5)	0.6309(4)	0.1562(3)
C(7)	−0.3627(4)	0.5437(4)	0.2133(3)
C(8)	−0.3964(3)	0.2513(4)	0.5005(2)
C(9)	−0.4574(4)	0.3472(4)	0.5176(3)
C(10)	−0.5519(4)	0.3494(4)	0.5749(3)
C(11)	−0.5850(4)	0.2551(5)	0.6163(3)
C(12)	−0.5267(4)	0.1583(4)	0.6001(3)
C(13)	−0.4325(4)	0.1566(4)	0.5433(3)
C(14)	−0.2382(4)	0.1053(3)	0.3425(3)
C(15)	−0.1676(4)	0.0193(4)	0.3742(4)
C(16)	−0.1585(5)	−0.0774(4)	0.3278(5)
C(17)	−0.2189(5)	−0.0891(4)	0.2469(5)
C(18)	−0.2909(6)	−0.0052(5)	0.2141(4)
C(19)	−0.3006(5)	0.0914(4)	0.2607(3)
C(20)	−0.0928(4)	0.3068(3)	0.4905(3)
C(21)	0.0110(4)	0.3428(4)	0.4530(3)
C(22)	0.1059(4)	0.3814(4)	0.5061(3)
C(23)	0.0980(4)	0.3816(4)	0.5970(3)
C(24)	0.0046(4)	0.3454(4)	0.6351(3)
C(25)	−0.1006(4)	0.3074(4)	0.5822(3)

3.2.5. In vitro screening

The in vitro tests were performed as described previously [27].

Acknowledgements

We thank Mrs. I. Verbruggen for recording the NMR spectra. We are grateful to Mr. H.J. Kolker, Dr. J.

Verweij, Professor Dr. G. Stoter and Dr. J.H.M. Schellens, Laboratory of Experimental Chemotherapy and Pharmacology, Department of Medical Oncology, Rotterdam Cancer Institute, NL-3008 AE Rotterdam, Netherlands for the in vitro tests. This research was supported by the Belgian Nationaal Fonds voor Wetenschappelijk Onderzoek (NFWO, Grant No. S2/5 CD F198, M.G.), the Belgian Fonds voor Kollektief Fundamenteel Onderzoek (FKFO, Grant No. 2.0094.94, R.W., M.B.), the Belgian Nationale Loterij (Grant No. 9.0006.93, R.W., M.B.), and the Human Capital and Mobility Programme of the European Union (Contract No. ERBCHRXCT920016). The Australian Research Council is thanked for support of the crystallographic facility.

References

[1] M. Gielen, A. El Khloufi, M. Biesemans and R. Willem, *Appl. Organomet. Chem., 7* (1992) 119; M. Gielen, A. El Khloufi, M. Biesemans, F. Kayser and R. Willem, *Appl. Organomet. Chem., 7* (1993) 201.
[2] M. Gielen, M. Biesemans, A. El Khloufi, J. Meunier-Piret, F. Kayser and R. Willem, *J. Fluorine Chem., 64* (1993) 279.
[3] M. Gielen, A. El Khloufi, D. de Vos, H.J. Kolker, J.H.M. Schellens and R. Willem, *Bull. Soc. Chim. Belg., 102* (1993) 761.
[4] M. Gielen, E.R.T. Tiekink, A. Bouhdid, D. de Vos, M. Biesemans, I. Verbruggen and R. Willem, *Appl. Organomet. Chem., 9* (1995) 639.
[5] M. Gielen, *Coord. Chem. Rev., 151* (1996) 41.
[6] R. Willem, A. Bouhdid, M. Biesemans, J.C. Martins, D. de Vos, E.R.T. Tiekink and M. Gielen, *J. Organomet. Chem., 514* (1996) 203.
[7] S.L. Foong, N.S. Weng, M. Gielen and V.G. Kumar Das, *Malaysian J. Sci., 15B* (1994) 13.
[8] K.C. Molloy, S.J. Blunden and R. Hill, *J. Chem. Soc., Dalton Trans.*, (1988) 1259.
[9] J. Holecek, M. Nadvornik, K. Handlir and A. Lycka, *J. Organomet. Chem., 241* (1983) 177.
[10] M. Gielen, A. El Khloufi, M. Biesemans, F. Kayser, R. Willem, B. Mahieu, D. Maes, J.N. Lisgarten, L. Wyns, A. Moreira, T.K. Chattopadhay and R. Palmer, *Organometallics, 13* (1994) 2849.
[11] R.C. Poller, *The Chemistry of Organotin Compounds*, Academic Press, New York, 1970.
[12] A.G. Davies and P.J. Smith, in G. Wilkinson (ed.), *Comprehensive Organometallic Chemistry*, Pergamon Press, Oxford, 1982, Chap. 11, p. 564.
[13] K.C. Molloy, K. Quill, S.J. Blunden and R. Hill, *Polyhedron, 5* (1986) 959.
[14] R.R. Holmes, R.O. Day, V. Chandrasekhar, J.F. Vollano and J.M. Holmes, *Inorg. Chem., 25* (1986) 2490.
[15] P.J. Smith, R.O. Day, V. Chandrasekhar and J.M. Holmes, *Inorg. Chem., 25* (1986) 2495.
[16] E.R.T. Tiekink, *Appl. Organomet. Chem., 5* (1991) 1; *Trends in Organomet. Chem., 1* (1994) 71.
[17] R. Willem, A. Bouhdid, F. Kayser, A. Delmotte, M. Gielen, J.C. Martins, M. Biesemans, B. Mahieu and E.R.T. Tiekink, *Organometallics, 15* (1996) 1920.
[18] H.O. Kalinowski, S. Berger and S. Braun, *Carbon-13 NMR Spectroscopy*, Wiley, Chichester, UK, 1988, pp. 200, 313–316.
[19] A. Bax and M.F. Summers, *J. Magn. Reson., 67* (1986) 565.
[20] M. Nadvornik, J. Holecek, K. Handlir and A. Lycka, *J. Organomet. Chem., 275* (1984) 43.
[21] A. Lycka, J. Holecek, M. Nadvornik and K. Handlir, *J. Organomet. Chem., 280* (1985) 323.
[22] J. Holecek, K. Handlir, M. Nadvornik and A. Lycka, *J. Organomet. Chem., 258* (1983) 147.
[23] E.R.T. Tiekink, M. Gielen, A. Bouhdid, M. Biesemans and R. Willem, *J. Organomet. Chem., 494* (1995) 247.
[24] A. Lycka, M. Nadvornik, K. Handlir and J. Holecek, *Collect. Czech. Chem. Commun., 49* (1984) 2903.
[25] I. Omae, *J. Organomet Chem. Lib., 21* (1989) 95.
[26] J. Mason, *Multinuclear NMR*, Plenum Press, New York, 1987, p. 627.
[27] Y.P. Keepers, P.E. Pizao, G.J. Peters, J. Van Ark-Otte, B. Winograd and H.M. Pinedo, *Eur. J. Cancer, 27* (1991) 897.
[28] F.A. Bovey, L. Jelinski and P.A. Mirau, *Nuclear Magnetic Resonance Spectroscopy*, Academic Press, San Diego, 2nd edn., 1987, Chap. 8, pp. 399–434.
[29] A. Sebald, in P. Diehl, E. Fluck, H. Günther, R. Kosfeld and J. Seelig (eds.), *Solid State NMR II: Inorganic Matter*, Springer, Berlin, 1994, p. 91.
[30] P.G. Harrison, in P.G. Harrison (ed.), *Chemistry of Tin*, Blackie, Glasgow, 1989, Chap. 3, p. 113.
[31] H.C.E. McFarlane, W. McFarlane and C.J. Turner, *Molec. Phys., 37* (1979) 1639.
[32] R. Willem, A. Delmotte, I. De Borger, M. Biesemans, M. Gielen and F. Kayser, *J. Organomet. Chem., 480* (1994) 255.
[33] TEXSAN, *Single Crystal Structure Analysis Software*, Molecular Structure Corp., TX, 1993.
[34] A.C.T. North, D.C. Phillips and F.S. Mathews, *Acta Crystallogr., A24* (1968) 351.
[35] M.C. Burla, M. Camalli, G. Cascarano, C. Giacovazzo, G. Polidori, R. Spagna and D. Viterbo, *J. Appl. Crystallogr., 22* (1989) 389.
[36] C.K. Johnson, ORTEP-II, *Report ORNL-5138*, Oak Ridge National Laboratory, Oak Ridge, TN, 1976.